Biodegradable Piezoelectric Force Sensor

Eli J. Curry[a], Kai Ke[b], Meysam T. Chorsi[b], Kinga S. Wrobel[b], Albert N. Miller III[b], Avi Patel[c], Insoo Kim[a,d], Jianlin Feng[e], Lixia Yue[e], Qian Wu[f], Chia-Ling Kuo[g], Kevin W.-H. Lo[a,h,i], Cato T. Laurencin[a,i,j], Horea Ilies[b], Prashant K. Purohit[k], and Thanh D. Nguyen[a,b,i,1]

[a]Department of Biomedical Engineering, University of Connecticut, Storrs, CT 06269; [b]Department of Mechanical Engineering, University of Connecticut, Storrs, CT 06269; [c]Department of Molecular and Cell Biology, University of Connecticut, Storrs, CT 06269; [d]Department of Medicine, University of Connecticut Health Center, Farmington, CT 06030; [e]Department of Cell Biology, University of Connecticut Health Center, Farmington, CT 06030; [f]Department of Pathology and Laboratory Medicine, University of Connecticut Health Center, Farmington, CT 06030; [g]Connecticut Institute for Clinical and Translational Science, Farmington, CT 06030; [h]Department of Medicine, Endocrinology, University of Connecticut Health Center, Farmington, CT 06030; [i]Institute for Regenerative Engineering, University of Connecticut Health Center, Farmington, CT 06030; [j]Department of Orthopedic Surgery, University of Connecticut Health Center, Farmington, CT 06030; and [k]Department of Mechanical Engineering and Applied Mechanics, University of Pennsylvania, Philadelphia, PA 19104

Edited by Daniel A. Heller, Memorial Sloan-Kettering Cancer Center, New York, NY, and accepted by Editorial Board Member Mark E. Davis December 12, 2017 (received for review June 15, 2017)

Measuring vital physiological pressures is important for monitoring health status, preventing the buildup of dangerous internal forces in impaired organs, and enabling novel approaches of using mechanical stimulation for tissue regeneration. Pressure sensors are often required to be implanted and directly integrated with native soft biological systems. Therefore, the devices should be flexible and at the same time biodegradable to avoid invasive removal surgery that can damage directly interfaced tissues. Despite recent achievements in degradable electronic devices, there is still a tremendous need to develop a force sensor which only relies on safe medical materials and requires no complex fabrication process to provide accurate information on important biophysiological forces. Here, we present a strategy for material processing, electromechanical analysis, device fabrication, and assessment of a piezoelectric Poly-L-lactide (PLLA) polymer to create a biodegradable, biocompatible piezoelectric force sensor, which only employs medical materials used commonly in Food and Drug Administration-approved implants, for the monitoring of biological forces. We show the sensor can precisely measure pressures in a wide range of 0–18 kPa and sustain a reliable performance for a period of 4 d in an aqueous environment. We also demonstrate this PLLA piezoelectric sensor can be implanted inside the abdominal cavity of a mouse to monitor the pressure of diaphragmatic contraction. This piezoelectric sensor offers an appealing alternative to present biodegradable electronic devices for the monitoring of intraorgan pressures. The sensor can be integrated with tissues and organs, forming self-sensing bionic systems to enable many exciting applications in regenerative medicine, drug delivery, and medical devices.

biodegradable | piezoelectric | PLLA | pressure | sensor

Measuring vital biophysiological pressures such as the pressure of diaphragmatic contraction, intraarticular pressure, intraabdominal pressure, intraocular pressure, intracranial pressure, etc. is important for monitoring health status, preventing the buildup of dangerous internal forces in impaired organs, and enabling novel approaches of using mechanical stimulation for tissue regeneration (1–3).

Pressure sensors are often required to be implanted and directly integrated with native soft tissues and organs. Therefore, the devices should be flexible and at the same time biodegradable to avoid an invasive removal surgery, which could damage directly interfaced tissues. In this regard, there have been achievements in degradable force sensors, relying on silicon piezoresistive probes or capacitive biopolymers (4, 5). These sensors exhibit excellent performance in monitoring biological pressures, including intracranial, abdominal, and cardiac pressures. However, for clinical applications, further improvements of these devices are still required to overcome some challenges including (*i*) the use of electronic materials (e.g., silicon and silicon dioxide), which has not been confirmed to be completely bioerodible and safe for long-term use inside the human body, (*ii*) the dependence on complex cleanroom fabrication tools, and (*iii*) the use of a battery to power passive materials. Ideally, erodible devices for biointegration should only contain materials which have been extensively studied and used in Food and Drug Administration (FDA)-approved implants. Recently, triboelectric sensors fabricated with biodegradable polymers have been reported with the exciting ability for in vivo energy harvesting (6). Friction-induced triboelectric charges, while ideal for energy harvesting and some force-detecting applications, are often susceptible to noise from motion of the sensor (7), variation of force response due to the delay of charge dissipation in the sensor (8), and a limitation of miniaturization due to the requirement of a physical gap between triboelectric layers.

Piezoelectricity is a phenomenon which allows materials to convert deformation into electricity and vice versa (9). Piezoelectric materials are often used for force/pressure sensors, transducers, and generators (10, 11). The materials can even be fabricated into nano- and microstructures and interfaced with soft tissues to monitor biological forces (9, 12–14). Since piezoelectric materials can generate electricity from mechanical impact (14), they can serve as appealing sensing materials, alternative to the described passive semiconductors and capacitive polymers, for self-powered force sensors. However, commonly used piezoelectric materials such

Significance

Measuring physiological pressures such as lung pressure, brain pressure, eye pressure, etc. is important for monitoring health status, preventing the buildup of dangerous internal forces in impaired organs, and enabling novel approaches of using mechanical stimulation for tissue regeneration. Pressure sensors are often implanted and directly integrated with soft biological systems. Therefore, the devices should be flexible and at the same time biodegradable to avoid invasive removal surgery. Here, we present the study and processing of a biodegradable polymer which can convert mechanical force to electricity, and employ the polymer to develop a biocompatible implanted force sensor. The sensor, relying solely on common medical materials, can monitor important biological forces and eventually self-vanish, causing no harm to the body.

Author contributions: E.J.C. and T.D.N. designed research; E.J.C., K.K., M.T.C., K.S.W., A.N.M., A.P., and T.D.N. performed research; I.K., J.F., L.Y., K.W.-H.L., C.T.L., H.I., P.K.P., and T.D.N. contributed new reagents/analytic tools; E.J.C., K.K., M.T.C., Q.W., C.-L.K., and T.D.N. analyzed data; I.K. consulted on electronics; and E.J.C., K.K., M.T.C., P.K.P., and T.D.N. wrote the paper.

The authors declare no conflict of interest.

This article is a PNAS Direct Submission. D.A.H. is a guest editor invited by the Editorial Board.

Published under the PNAS license.

[1]To whom correspondence should be addressed. Email: nguyentd@uconn.edu.

This article contains supporting information online at www.pnas.org/lookup/suppl/doi:10.1073/pnas.1710874115/-/DCSupplemental.

ENGINEERING

Downloaded at Palestinian Territory, occupied on November 27, 2021

www.manaraa.com

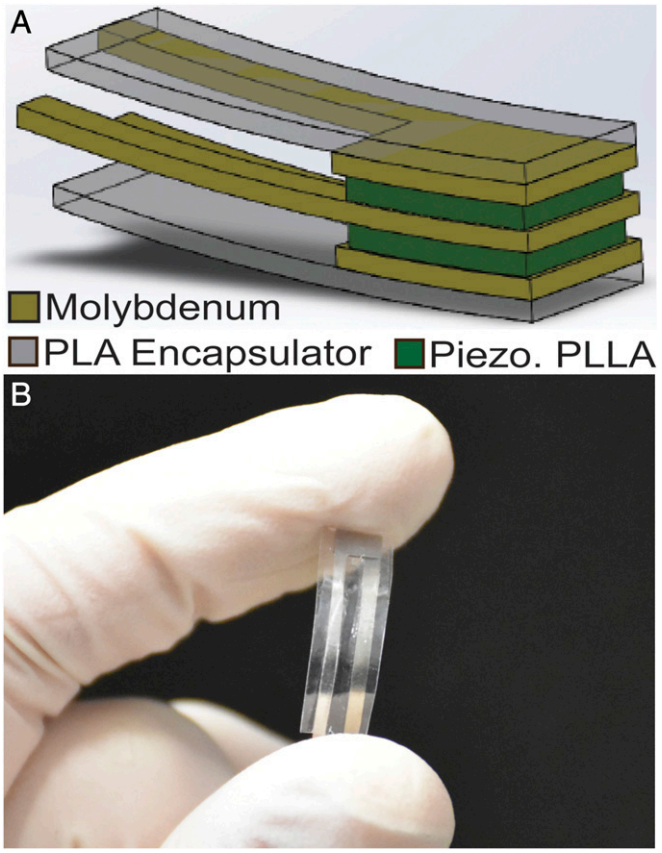

Fig. 1. Biodegradable piezoelectric PLLA pressure sensor. (*A*) Simplified schematic representing the biodegradable piezoelectric PLLA sensor. (*B*) Optical image of a fabricated biodegradable piezoelectric PLLA sensor (5 mm × 5 mm and 200 μm thick).

as lead zirconate titanate (PZT) and polyvinylidene difluoride (PVDF) contain toxic or nonbiodegradable components, respectively, and thus are not favorable for implantation inside the human body. Poly-L-lactic acid (PLLA), a biodegradable polymer used extensively in FDA-approved implants, has recently been found to exhibit piezoelectricity when appropriately processed (15–17). The material exhibits shear piezoelectricity due to electrical polarity present in the carbon–oxygen double-bond branching off from the polymer backbone chain (18, 19). Although possessing a modest piezoelectric response (5–15 pC/N), PLLA has a low dielectric constant, which allows the material to perform the same energy-conversion efficacy as the common piezoelectric polymer PVDF (16, 20). By creating multilayers, one can achieve even higher piezoelectricity from PLLA, with an "effective" conversion efficiency, similar to that of ceramic PZT (21).

Here, we present a strategy for material processing, electromechanical analysis, device fabrication, and assessment of a piezoelectric Poly-L-lactide (PLLA) polymer to create a biodegradable, biocompatible piezoelectric force sensor which only employs medical materials used commonly in FDA-approved implants, for the monitoring of biological forces such as the pressure of diaphragmatic contraction.

Fig. 1*A* illustrates the sensor structure, which includes two layers of piezoelectric PLLA, sandwiched between molybdenum (Mo) or magnesium (Mg) electrodes and encapsulating layers of polylactic acid (PLA). Mg and Mo are used for implanted cardiovascular stents (22, 23) while PLA and PLLA are often used for bone screws and tissue scaffolds (24, 25). The device dimensions are only 5 mm × 5 mm and 200 μm thick, thereby allowing the sensor to be flexible (Fig. 1*B*). This biodegradable piezoelectric sensor will offer an extremely useful tool to monitor vital biological pressures. While bulk moduli of the materials in the sensor are generally large (*SI Appendix*, Table S1), the sensor's thickness can be reduced, making it even more flexible and facilitating device integration with soft tissues and organs to form a self-sensing bionic system (26). This will enable many applications in regenerative medicine, drug delivery, and medical devices.

To make PLLA piezoelectric, the two major material properties that need to be improved are the crystallinity and orientation degree of the polymer chains (20). The net polarization, appearing in PLLA under applied force, is due to the relative alignment of the carbon–oxygen double bonds (C=O) branching out from the PLLA backbone. In normal conditions (without applied force), all polarizations from the C=O bonds along a PLLA polymeric chain are canceled out but shear stress will align and direct these polarizations more in one direction, generating a nonzero out-of-plane polarization in a single polymeric chain. To obtain a net polarization over a bulk PLLA film, these polymeric chains need to be oriented in the same direction from aligned crystalline domains. The mechanism of shear piezoelectricity for polymers with chiral structures has been well-described in previous reports (20, 27). The improvement of crystallinity and alignment is performed by thermal annealing and mechanical stretching processes, respectively. While PLLA can be transformed into a piezoelectric material through other processes like electrospinning, the inherently rough surface of a nanofiber film potentially causes unwanted triboelectric error and inconsistent readings in sensing applications (28). We first create a thin PLLA film by heat compression. The film is then mechanically stretched (*SI Appendix*, *Methods*) at an annealing temperature of 90 °C. The initial length of the PLLA film is then compared with the final stretched length to determine the draw ratio. Fig. 2*A* describes the one-dimensional X-ray diffraction (XRD) of stretched PLLA films with different draw ratios (DRs). The processed PLLA often exhibits three crystalline orientations of [111], [200], and [110] (29), yet once the films reach a DR of 3.5, the (111) crystal face disappears and, at the same time, the intensity of the (200) and (110) peaks increases. This represents a change from the α-form crystal structure, which has a left-handed 10_3 helical conformation, to the β-form crystal structure, which has a 3_1 helical conformation (30). In other words, the crystalline domains are oriented or aligned more in the [200] and [110] directions under a large stretching force. Additionally, from the XRD data, the crystallinity degree for the PLLA films with different DRs could be quantified, based on the ratio of the area underneath the [200] and [110] peaks to the area underneath the entire curve, as seen in Fig. 2*A* (*Inset*). The data show the crystallinity percentage of the PLLA films increases with increasing DR up to ∼5. Once a larger DR is employed, a clear downward trend is seen. Likewise, the stretching with larger DRs improves orientation degree of the crystal domains, as seen in the 2D XRD image of Fig. 2*B*, and provides the maximal alignment of crystal domains (quantified through Herman's orientation factor as seen in *SI Appendix*, Table S2) at the DR ∼5. These results explain an optimal DR (∼5) to obtain the best piezoelectric effect, as previously reported (15).

For our ultimate goal of using shear piezoelectricity in the PLLA to sense normal out-of-plane stress, the PLLA film needs to be further processed to translate the normal stress into in-plane shear, which is the driving force for piezoelectric outputs (31). By deriving a mechanical model based on the constitutive shear piezoelectric equations, we can obtain a relationship between the out-of-plane normal stress and the in-plane shear as well as the resulting electrical field across the two major top and bottom surfaces of the PLLA film, upon applied normal stresses. Details of the theoretical calculation are described in *SI Appendix*. Our theoretical derivation shows a linear relationship between voltage output and applied force, and that the PLLA film with a

Downloaded at Palestinian Territory, occupied on November 27, 2021
www.manaraa.com

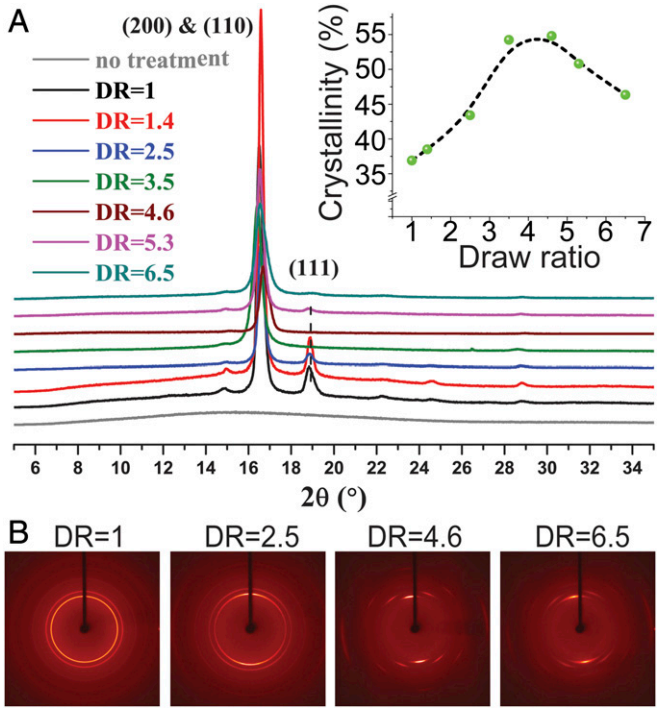

Fig. 2. Characterization of crystallinity and polymer chain orientation for processed PLLA. (*A*) Results from one-dimensional (1D) XRD of stretched PLLA films with different DRs. (*Inset*) Crystallinity percentage of the processed PLLA for different DRs, quantified from the 1D XRD spectrum. (*B*) Two-dimensional XRD images show polymer chain's orientation of the stretched PLLA films with different DRs.

cutting angle of 45°, relative to the stretching direction, exhibits the maximal piezoelectric output in both impact and vibration modes. These theoretical analyses are also supported by experimental results (*SI Appendix* and *SI Appendix*, Figs. S1–S7). Therefore, we cut the PLLA film at an angle of 45°, relative to the stretching direction for all sensing devices developed later on (16). For convention, a "treated" PLLA is a film which has gone through an annealed stretching process and a 45° cutting, while a "processed" PLLA is a film which has only gone through annealed stretching.

We then assess piezoelectric outputs of the treated PLLA films under mechanical strains/forces through vibration and impact testing. Both procedures have been employed for the characterization of other piezoelectric materials (32, 33). Fig. 3*A* provides simplified diagrams illustrating the two procedures utilized.

In the vibration system, a film made of the treated PLLA, sandwiched between aluminum foil electrodes and encapsulated in Kapton tape (*SI Appendix*, *Methods*), is tightly affixed to the middle of the top portion of a polycarbonate beam with Kapton tape. Kapton tape is used to minimize any errors in signal measurement due to triboelectric effects. Note that we used nondegradable materials for electrodes and encapsulators to characterize piezoelectricity of PLLA with different draw ratios due to their easy fabrication, flexibility, and durability while functional-sensing devices described later will be made of completely bioresorable materials. All of the sensors used in this experiment have the same area of 161.29 mm^2, with the thickness of each sample decreasing with increasing DR. The thicknesses of the PLLA samples used are 29, 68, 46, 27, and 20 μm for the 0 (unstretched), 1, 2.5, 4.6, and 6.5 DR samples, respectively. One end of the beam is fixed and the other end of the beam is attached to an actuator which can be controlled to move at a desired frequency and amplitude (*SI Appendix*, *Methods*). This results in the beam oscillating up and down, thus subjecting the PLLA sensor to mechanical strains (Fig. 3*A*, *Left*). In

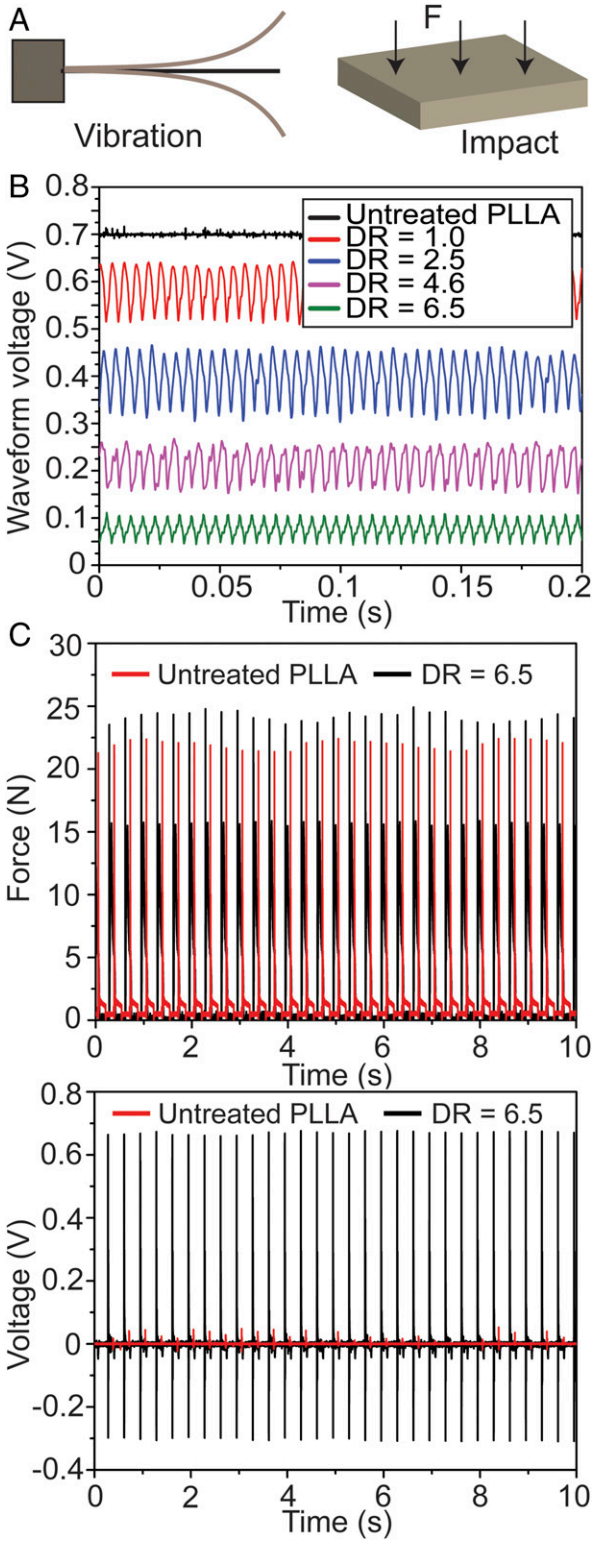

Fig. 3. Characterization of piezoelectric PLLA output from vibration and impact modes. (*A*) Simplified schematics representing the vibration (*Left*) and impact (*Right*) methods used to characterize the PLLA. F, force. (*B*) Voltage output from the treated PLLA with different DRs under a vibration at 200 Hz. (*C*) Voltage output from an untreated PLLA (red) and treated PLLA (black, DR = 6) (*Bottom*) under the same impact force (*Top*).

Downloaded at Palestinian Territory, occupied on November 27, 2021
ENGINEERING
www.manaraa.com

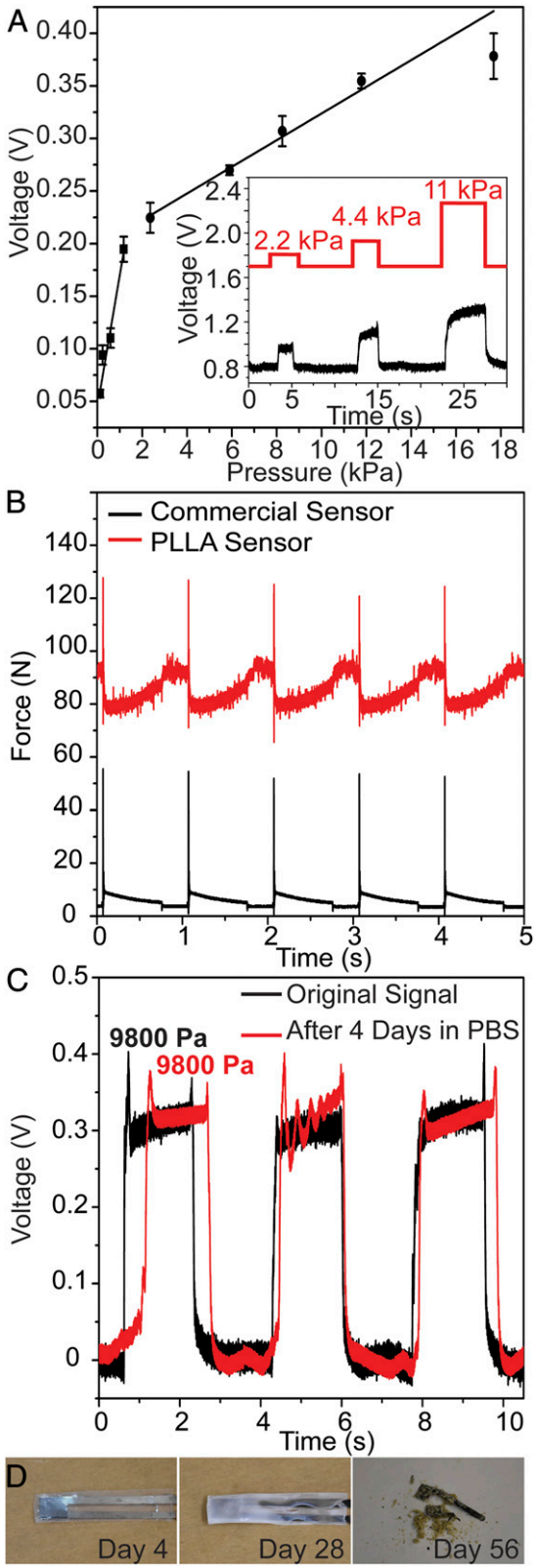

Fig. 4. Characterization of biodegradable piezoelectric PLLA sensor. (*A*) Typical calibration curve generated by a PLLA sensor/charge amplifier circuit assembly. (*Inset*) Typical output voltage signals from different input forces. (*B*) Output signals from the biodegradable PLLA sensor (red) and a commercially available piezoelectric quartz sensor (black) under the same applied force/pressure. (*C*) Output voltages of the PLLA sensor under the same applied pressure on the initial day and after 4 d in phosphate-buffered solution at 37 °C. (*D*) Optical images showing the sensor at different days in the buffered solution at an accelerated-degradation temperature of 74 °C.

the impact system, the same actuator is affixed with a dynamic force sensor and driven by a defined voltage waveform to apply consistent normal forces on the PLLA sensor (Fig. 3*A*, *Right* and *SI Appendix*, *Methods*). In both testing methods, the voltage output is measured by an oscilloscope. Fig. 3*B* illustrates open-circuit voltage outputs from PLLA films of different DRs subjected to a 200-Hz vibration force that resulted in an elongation strain of about 6×10^{-6} (measured by a strain gauge; *SI Appendix*, Fig. S8). The signal generated from the four treated PLLA samples of different DRs clearly shows piezoelectric waveform outputs with the same frequency as that of the mechanical input (200 Hz) while the untreated PLLA film (control sample) resulted in only noise. While the data show the sample with a DR of 2.5 has the largest signal output, it is not conclusive that this is an optimal DR. The sample thicknesses, due to mechanical stretching, are not precisely controlled, thus the mechanical properties and resonant frequencies of each film are expected to be different. Further illustration of the PLLA film's voltage changing with frequency is illustrated in *SI Appendix*, Fig. S9. Fig. 3*C* illustrates a typical open-circuit voltage output from the impact testing of a treated PLLA film with DR of ~6.5. An input force of ~23 N (about 1.4 kPa) resulted in a peak-to-peak voltage output of 0.9 V from the treated PLLA, while a nontreated PLLA resulted in only noise. The piezoelectric outputs increased with increasing applied force in a linear manner (*SI Appendix*, Fig. S3).

Using reported mechanical properties of PLLA and our aforementioned model, we can roughly estimate a piezoelectric constant d_{14} of ~11 pC/N and obtain a good fit between experimental data and theoretical calculations for both the impact and vibration modes (see details in *SI Appendix* and *SI Appendix*, Figs. S3 and S6). The same modeling results, obtained from two independent experiments, and the consistency between experimental and theoretical calculations validate our mechanical model and reinforce the estimated d_{14}, which is also in the range of previous reports (17).

After confirming piezoelectricity in the treated PLLA, we then fabricate a biodegradable PLLA-based force sensor. The biodegradable sensor is fabricated using a combination of the piezoelectric PLLA, molybdenum electrodes, and encapsulating PLA layers. The treated piezoelectric PLLA film has an area of 5×5 mm^2 and a thickness of 27 μm. The molybdenum electrodes are cut out of a sheet and affixed to the top and bottom of the PLLA film. Care has to be taken to ensure the electrodes are not shorted together. The PLLA/Mo assembly is then sandwiched between sheets of PLA. If higher sensitivity is needed, more piezoelectric PLLA layers will be added to fabricate a multilayer device (*SI Appendix*, Figs. S10 and S11). The PLA encapsulating layers are initially sealed together using a biodegradable PLLA glue (*SI Appendix*, *Methods*). The PLA encapsulator is then thermally sealed by using a commercial plastic sealer (*SI Appendix*, *Methods*) at a temperature of ~200 °C for 4 s.

After the fabrication process, we assess the sensitivity of this biodegradable piezoelectric PLLA sensor. The relatively low and bipolar output voltage (i.e., including negative and positive peaks) of PLLA is not ideal for use to visualize force response. Therefore, a charge amplifier circuit (*SI Appendix*, Fig. S12) was built to convert the force-induced charge into an easy-to-visualize voltage signal. By placing different predefined weights on the sensor, different known forces/pressures are applied on the device to calibrate the voltage output. As can be seen from the Fig. 4*A* (*Inset*), there are clearly distinguishable peaks for different magnitudes of input forces. Additionally, under the same applied pressure, the sensor generated a defined and consistent voltage pulse as seen in *SI Appendix*, Fig. S13. The clear and distinguishable signals allowed us to construct a calibration curve (Fig. 4*A*). This calibration curve could be divided into two linear regions which are usable for

Downloaded at Palestinian Territory, occupied on November 27, 2021
www.manaraa.com

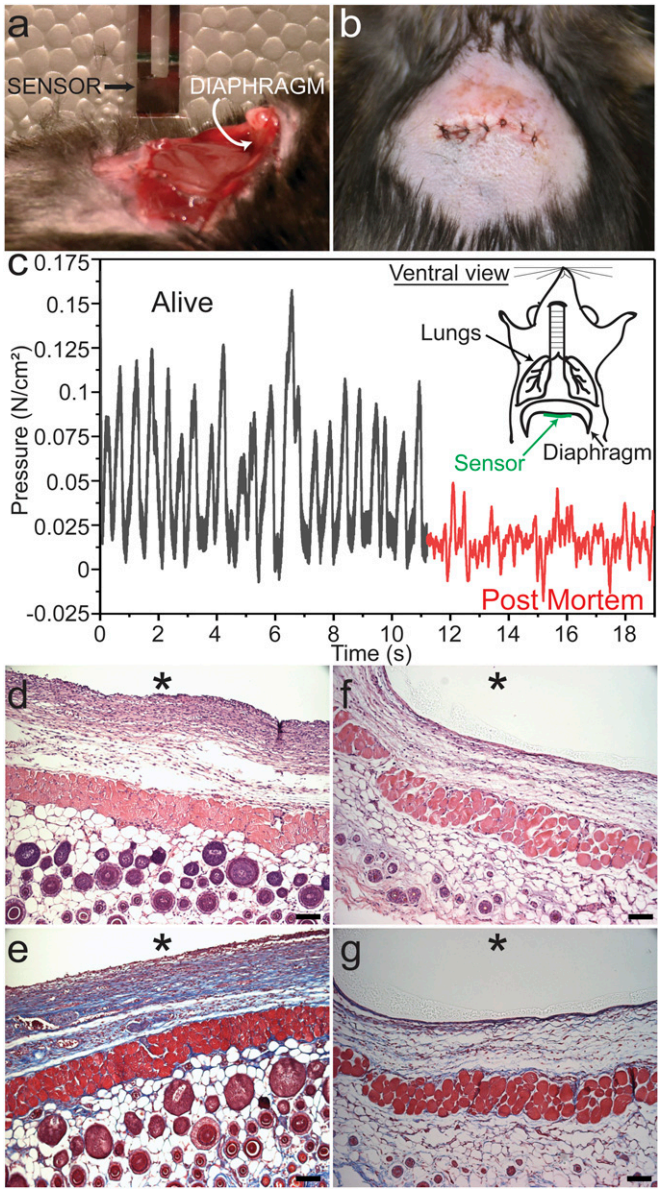

Fig. 5. In vivo force measurement and biocompatibility test. (*A*) Optical image illustrates the sensor and a mouse abdominal cavity with diaphragmatic membrane. (*B*) Surgical wound closed up by medical suture on abdomen of the mouse, which received an implanted PLLA sensor. (*C*) Data show the distinct force signals generated by the implanted sensor when the mouse was alive and under anesthesia (black), and when the mouse was euthanized by overdose of anesthetics (red). (*Inset*) Diagram describes the sensor attached to the bottom of mouse diaphragm inside the abdomen. (*D*–*G*) Histology images of s.c.-implanted PLLA sensors after 2 and 4 wk, respectively. *D* and *F* are histology stained by H&E while *E* and *G* are histology stained by Masson's Trichrome. Asterisks (*) show locations of the implanted sensors. (Scale bars, 100 μm.)

measuring pressures in the wide range of 0–18 kPa. This pressure range is relevant to many important biophysiological pressures. Examples include intracranial pressure (from 0 to 2.7 kPa) (4), intraocular pressure (from 0 to 5.3 kPa) (1), etc.

We then evaluate accuracy of our sensor by comparing the device's reading with a commercially available piezoelectric quartz force sensor (208C02; PCB Piezotronics). To do this, our sensor is first calibrated as previously described in this article. Next the PLLA sensor is affixed to a beam and covered with an aluminum plate in our impact-testing device (*SI Appendix*, *Methods*), taking great care to prevent triboelectric signal error by sandwiching the sensor in between sheets of PLA. Using the calibration curve developed for this sensor, the voltage output from the charge amplifier circuit is then converted to a force value. As can be seen in Fig. 4*B*, the resulting signal closely represents the magnitude of impact force measured by the commercial sensor. The only major difference in signals is the inverted nature of our sensor, which is due to the inverting nature of the charge amplifier circuit. The accuracy of the sensor was also confirmed under 10,000 cycles of a 2-kPa and 1-MPa force (*SI Appendix*, Fig. S14), ensuring reliability for long-term measurements.

After verifying the accuracy of our sensor, the next goal was to show its viability during degradation. As the biodegradable nature of the PLA, Mo, and PLLA would suggest, it is important to show the sensor can physically degrade. However, the sensor should maintain its ability to measure force during some portion of its degradation lifespan for use in various applications in vivo. We place the sensor in PBS at the physiological temperature 37 °C and recalibrate the device every 24 h. Fig. 4*C* illustrates the sensor's typical output signals before and after 4 d of degradation. Under the same applied pressure (9.8 kPa), the magnitude of the sensor's signal output is still the same after 4 d. This result was also confirmed in vivo by s.c. implanting the sensor into the backs of mice for a period of 2, 4, 8, and 16 d (*SI Appendix*, Figs. S15 and S16). The 4-d period is relevant to the use of this biodegradable sensor in the monitoring of important physiological pressures such as intracranial pressures in patients with acute traumatic brain injuries (34). Eventually, the sensor completely degrades and breaks down. This can be visualized after a 56-d period in an accelerated degradation process at 74 °C (Fig. 4*D*). Different thicknesses of the PLA encapsulators result in different degradation times (*SI Appendix*, Fig. S17). Therefore, longer functional lifetimes of this sensor can be obtained by engineering the thickness. Other parameters such as molecular weight can also be used to engineer degradation of the PLA encapsulating layer. This lifetime can be predefined in vitro before the implantation process. Surface-erodible biodegradable polymers such as polyorthoester, polyanhydride, polyglycerol sebacate, etc. can be used instead of PLA to precisely control and engineer the device's functional lifetime.

As a proof of concept for the sensor's application, we employed the device to measure the pressure of diaphragmatic contraction in a mouse to detect the breathing pattern of the animal in vivo. The sensor, coated with a very thin layer of medical glue, is inserted into a small incision (8 mm) which is made below the mouse's diaphragm in the abdomen, as seen in Fig. 5*A*. The sensing patch alone is small (5 × 5 mm), allowing a complete suture of the opened wound, as seen in Fig. 5*B*. In the measurement, small Mo/PLA wires from the sensing patch were run through the sutured wound into an external charge amplifier circuit connected to an oscilloscope to measure electrical voltage. After letting the mouse rest for 15 min postsurgery, a clearly distinguishable signal (Fig. 5*C*) was observed while the anesthetized mouse was breathing under normal anesthesia, and the signal was completely suppressed after the animal was euthanized by an overdose of anesthetics. The signal generated from the mouse, when alive, has a frequency of (~2 Hz) and correlates to an input force of (~0.1 N/cm^2 or ~1 kPa). Both of these measurement results are consistent with previously reported respiration rates in mice (35). Additionally, the sensor was also able to detect abnormal breathing after anesthesia overdose until the moment the animal was deceased. This "agonal" breathing has a lower frequency and larger pressure, which is likely due to the uptake of more oxygen (*SI Appendix*, Fig. S18). The measured pressure signal was then compared to the signal generated by a nontreated PLLA sensor to verify the signal was not generated by triboelectricity and motion artifacts of the wires (*SI Appendix*, Fig. S19). These results clearly illustrate the sensor's ability to measure physiological forces and a potential use of the

Downloaded at Palestinian Territory, occupied on November 27, 2021
www.manaraa.com

sensor for monitoring respiratory disorders caused by obstructive pulmonary diseases (36).

To verify the sensor's biocompatibility, we implanted the sensor into an s.c. area on the back of mice (*SI Appendix*, Fig. S20), which is rich with immune cells and often used for testing biocompatibility. The implants are then taken out at 2 and 4 wk. We perform histological analysis by staining prepared tissue slides (*SI Appendix*, *Methods*) with hematoxylin and eosin (H&E) to observe inflammatory cells, and Masson's Trichrome blue to detect fibrosis, as depicted in Fig. 5 *D*–*G* and *SI Appendix*, Fig. S21. We also performed immunohistochemical stains with CD64 antibody to reveal macrophages (*SI Appendix*, Fig. S21). The histological images show only a mild immune reaction without significant presence of inflammation, multinucleated giant cells, and fibrous capsules. Mild fibrosis and activated macrophages are seen at 2 wk, but remarkably reduced to normal levels at 4 wk.

Conclusions

We present a strategy for material processing, characterization, electromechanical analysis, and device fabrication of biodegradable piezoelectric PLLA to create a biodegradable piezoelectric force sensor to monitor important physiological forces. The sensor has a wide range of measurable pressures and can be implanted anywhere in the body with minimal immune response due to the sensor's ability for miniaturization and the biocompatible and biodegradable nature of the materials used. Additionally, the simple fabrication process, compared with photolithography-assembled sensors, makes the sensor more favorable. The PLLA sensor relies on piezoelectricity, which allows the device to generate electrical output upon applied force, and therefore, in principle, we could eliminate the use of a battery to power this device. As we showed the PLLA sensor can be implanted into the abdomen of a mouse to measure the pressure of diaphragmatic contraction, we anticipate many other applications of this sensor for biointegration, enabling the development of a new class of organs and tissues with the ability of self-monitoring. Furthermore, the piezoelectricity of PLLA could be employed to harvest energy from alternative biological deformations (e.g., the beating of heart, lung, etc.) to produce useful electrical stimulation for tissue repair/regeneration, while the material will be degraded to facilitate the tissue-regeneration process. Several improvements can be made to the current sensor design, including implementation of a wireless transmitter, creating a fully implanted system and improvement of piezoelectricity to reduce the sensor dimensions for further miniaturization. Nevertheless, this sensor, only made of common biomedical materials, is a significant step forward for the field of implantable force sensors and offers an appealing alternative to the present biodegradable electronic devices for monitoring a variety of important biophysiological pressures such as the pressure of diaphragmatic contraction, intraarticular pressure, intraabdominal pressure, intraocular pressure, intracranial pressure, etc.

Materials and Methods

Details of fabrications and characterizations of the PLLA and the force sensor along with in vitro and in vivo experiments all appear in *SI Appendix*. Animal procedures are approved and performed following Institutional Animal Care and Use Committee guidelines at the University of Connecticut Health Center.

ACKNOWLEDGMENTS. The authors thank Jeffrey Baroody for proofreading the manuscript. We thank Dr. Daniela Morales for assistance with XRD. We thank Dr. Liping Wang, Dr. Xiaonan Xin, Zhihua Wu, and Zhifang Hao for the animal surgery and histology. We thank Dr. Mario F. Perez for consulting on the in vivo pressure measurement. The research is supported by NIH Grant 1R21EB024787, Academic Plan Award (University of Connecticut), and Hartford Engineering a Limb project.

1. Bello SA, Malavade S, Passaglia CL (2017) Development of a smart pump for monitoring and controlling intraocular pressure. *Ann Biomed Eng* 45:990–1002.
2. Jayson MI, Dixon AS (1970) Intra-articular pressure in rheumatoid arthritis of the knee. 3. Pressure changes during joint use. *Ann Rheum Dis* 29:401–408.
3. Talmor D, et al. (2008) Mechanical ventilation guided by esophageal pressure in acute lung injury. *N Engl J Med* 359:2095–2104.
4. Kang S-K, et al. (2016) Bioresorbable silicon electronic sensors for the brain. *Nature* 530:71–76.
5. Boutry CM, et al. (2015) A sensitive and biodegradable pressure sensor array for cardiovascular monitoring. *Adv Mater* 27:6954–6961.
6. Zheng Q, et al. (2016) Biodegradable triboelectric nanogenerator as a life-time designed implantable power source. *Sci Adv* 2:e1501478.
7. Zi Y, et al. (2015) Triboelectric-pyroelectric-piezoelectric hybrid cell for high-efficiency energy-harvesting and self-powered sensing. *Adv Mater* 27:2340–2347.
8. Seol M-L, Han J-W, Moon D-I, Meyyappan M (2017) Hysteretic behavior of contact force response in triboelectric nanogenerator. *Nano Energy* 32:408–413.
9. Qi Y, et al. (2011) Enhanced piezoelectricity and stretchability in energy harvesting devices fabricated from buckled PZT ribbons. *Nano Lett* 11:1331–1336.
10. Chengkuo L, Itoh T, Suga T (1996) Micromachined piezoelectric force sensors based on PZT thin films. *IEEE Trans Ultrason Ferroelectr Freq Control* 43:553–559.
11. Chee CW, Wong CH, Dahari Z (2016) An investigation of array of piezoelectric transducer for raindrop energy harvesting application. *2016 IEEE Region Tenth Conference (TENCON)* (IEEE, New York), pp 3771–3774.
12. Nguyen TD, et al. (2012) Piezoelectric nanoribbons for monitoring cellular deformations. *Nat Nanotechnol* 7:587–593.
13. Nguyen TD, et al. (2010) Wafer-scale nanopatterning and translation into high-performance piezoelectric nanowires. *Nano Lett* 10:4595–4599.
14. Qi Y, Nguyen TD, Purohit PK, McAlpine MC (2012) Stretchable piezoelectric nanoribbons for biocompatible energy harvesting. *Stretchable Electronics*, ed Someya T (Wiley-VCH, Weinheim, Germany), pp 111–139.
15. Eiichi F (1998) New piezoelectric polymers. *Jpn J Appl Phys* 37:2775–2780.
16. Masamichi A, Hideki K, Keisuke K, Yoshiro T (2012) Film sensor device fabricated by a piezoelectric poly(L-lactic acid) film. *Jpn J Appl Phys* 51:09LD14.
17. Tajitsu Y, Kawai S, Kanesaki M, Date M, Fukada E (2004) Microactuators with piezoelectric polylactic acid fibers—toward the realization of tweezers for biological cells. *Ferroelectrics* 304:195–200.
18. Sawano M, Tahara K, Orita Y, Nakayama M, Tajitsu Y (2010) New design of actuator using shear piezoelectricity of a chiral polymer, and prototype device. *Polym Int* 59:365–370.
19. Ando M, et al. (2013) Pressure-sensitive touch panel based on piezoelectric poly (l-lactic acid) film. *Jpn J Appl Phys* 52:09KD17.
20. Yoshida M, Onogi T, Onishi K, Inagaki T, Tajitsu Y (2014) High piezoelectric performance of poly (lactic acid) film manufactured by solid-state extrusion. *Jpn J Appl Phys* 53:09PC02.
21. Yoshida T, et al. (2011) Piezoelectric motion of multilayer film with alternate rows of optical isomers of chiral polymer film. *Jpn J Appl Phys* 50:09ND13.
22. Di Mario C, et al. (2004) Drug-eluting bioabsorbable magnesium stent. *J Interv Cardiol* 17:391–395.
23. Stinson JS (1999) US Patent 5891191A.
24. Bos RR, Boering G, Rozema FR, Leenslag JW (1987) Resorbable poly(L-lactide) plates and screws for the fixation of zygomatic fractures. *J Oral Maxillofac Surg* 45:751–753.
25. Liu C, Xia Z, Czernuszka J (2007) Design and development of three-dimensional scaffolds for tissue engineering. *Chem Eng Res Des* 85:1051–1064.
26. Nguyen TD, Timko BP (2017) Bionics in tissue engineering. *Tissue Engineering for Artificial Organs* (Wiley-VCH, Weinheim, Germany), pp 677–699.
27. Minary-Jolandan M, Yu M-F (2009) Nanoscale characterization of isolated individual type I collagen fibrils: Polarization and piezoelectricity. *Nanotechnology* 20:085706.
28. Syuhei I, et al. (2012) Sensing using piezoelectric chiral polymer fiber. *Jpn J Appl Phys* 51:09LD16.
29. Xu H, Teng C, Yu M (2006) Improvements of thermal property and crystallization behavior of PLLA based multiblock copolymer by forming stereocomplex with PDLA oligomer. *Polymer (Guildf)* 47:3922–3928.
30. Ru J-F, et al. (2016) Dominant β-form of poly(l-lactic acid) obtained directly from melt under shear and pressure fields. *Macromolecules* 49:3826–3837.
31. Masamichi A, et al. (2013) Pressure-sensitive touch panel based on piezoelectric poly(L-lactic acid) film. *Jpn J Appl Phys* 52:09KD17.
32. Saravanos DA, Heyliger PR, Hopkins DA (1997) Layerwise mechanics and finite element for the dynamic analysis of piezoelectric composite plates. *Int J Solids Struct* 34:359–378.
33. Guo Q, Cao GZ, Shen IY (2013) Measurements of piezoelectric coefficient d33 of lead zirconate titanate thin films using a mini force hammer. *J Vib Acoust* 135:011003.
34. Maloney PR, et al. (2016) Intracranial pressure monitoring in acute liver failure: Institutional case series. *Neurocrit Care* 25:86–93.
35. Ewald AJ, Werb Z, Egeblad M (2011) Monitoring of vital signs for long-term survival of mice under anesthesia. *Cold Spring Harb Protoc* 2011:pdb.prot5563.
36. Sinderby C, et al. (2001) Diaphragm activation during exercise in chronic obstructive pulmonary disease. *Am J Respir Crit Care Med* 163:1637–1641.

Downloaded at Palestinian Territory, occupied on November 27, 2021
www.manaraa.com